frontiers | Frontiers in Materials

TYPE Original Research
PUBLISHED 30 January 2023
DOI 10.3389/fmats.2022.1100036

Check for updates

OPEN ACCESS

EDITED BY
Her-Hsiung Huang,
National Yang Ming Chiao Tung University, Taiwan

REVIEWED BY
Deng-Guang Yu,
University of Shanghai for Science and Technology, China
Ghasem Sargazi,
Bam University of Medical Sciences and Health Services, Iran

*CORRESPONDENCE
Mohammed H. Geesi,
m.geesi@psau.edu.sa

SPECIALTY SECTION
This article was submitted to Environmental Degradation of Materials, a section of the journal Frontiers in Materials

RECEIVED 16 November 2022
ACCEPTED 14 December 2022
PUBLISHED 30 January 2023

CITATION
Geesi MH, Jalil AT, Riadi Y, Aljohani TA and Alameri AA (2023), Hybrids of SiO_2 substrate and electrospun Ni-MOF/polysulfone fibers for an efficient removal of CH4 gas pollution. *Front. Mater.* 9:1100036. doi: 10.3389/fmats.2022.1100036

COPYRIGHT
© 2023 Geesi, Jalil, Riadi, Aljohani and Alameri. This is an open-access article distributed under the terms of the Creative Commons Attribution License (CC BY). The use, distribution or reproduction in other forums is permitted, provided the original author(s) and the copyright owner(s) are credited and that the original publication in this journal is cited, in accordance with accepted academic practice. No use, distribution or reproduction is permitted which does not comply with these terms.

Hybrids of SiO_2 substrate and electrospun Ni-MOF/polysulfone fibers for an efficient removal of CH4 gas pollution

Mohammed H. Geesi[1]*, Abduladheem Turki Jalil[2], Yassine Riadi[3], Talal A. Aljohani[4] and Ameer A. Alameri[5]

[1]Department of Chemistry, College of Science and Humanities in Al-Kharj, Prince Sattam Bin Abdulaziz University, Al-Kharj, Saudi Arabia, [2]Medical Laboratories Techniques Department, Al-Mustaqbal University College, Hillah, Iraq, [3]Department of Pharmaceutical Chemistry, College of Pharmacy, Prince Sattam Bin Abdulaziz University, Al-Kharj, Saudi Arabia, [4]Materials Science Research Institute, King Abdulaziz City for Science and Technology, Riyadh, Saudi Arabia, [5]Department of Chemistry, University of Babylon, Hillah, Iraq

In this study, novel nanostructures based on Ni-MOF/polysulfone nanofibers were fabricated by microwave-assisted electrospinning method. The final Ni-MOF/polysulfone fibrous nanostructure were immobilized on SiO_2 substrates with high physicho-chemical properties. These nanostructures with an average diameter of 20 nm and a specific surface area of 1690 m^2/g were used as novel adsorption for CH_4 gas adsorption. It seems that the integration of novel Ni-MOF compounds into the fibrous network has differentiated these materials from previous samples. Since the experimental parameters significantly affect the specific surface area, the parameters including voltage, concentration, and distance between the collector and source are designed by the fractional factorial method. The results were optimized by contour plots, ANOVA and surface plots, theoretically. The results show that the sample has an adsorption rate of about 5.14 mmoL/g. The improved CH_4 gas adsorption performance is attributed to the large specific surface area and porous nature of the Ni-MOF/Ps nanostructure which is more convenient and accessible for CH4 gas adsorption.

KEYWORDS

Ni-MOF, Ps nanofibrous polymer, SiO2 substrate, gas adsorption, systematic study

1 Introduction

Air pollution crises have become a global problem in all dimensions with dangerous effects (Zhao et al., 2021a; Han et al., 2022; Nazar and Niedoszytko, 2022). This problem, which has spread day by day, has affected humans, the environment, animals and plants. Although these gases have different categories, the most effects can be attributed to greenhouse gases (Jerrett et al., 2005; Glencross et al., 2020; Zhao et al., 2023).

Methane (CH_4) is one of the most common examples of greenhouse gases, whose harmful effects are tangible in the last few years (Klewiah et al., 2020). So far, various

compounds such as nanoparticles, zeolite, activated carbon and nanofibers were used for CH_4 gas adsorption (Conte et al., 2020; Karimi et al., 2021). Although these compounds have capabilities in the field of CH_4 gas adsorption, their efficiency is not ideal for adsorption applications (Zuo et al., 2022).

One of the important and influential parameters on gas adsorption is the specific surface area. Therefore, the introduction of novel compounds with a high specific surface can affect the adsorption processes of the sample (Okolo et al., 2015).

Nanofibers are efficient nanostructures with distributed properties due to high specific surface area, significant thermal stability, and small particle size distribution (Fischer, 2018). By using electrospinning, it is possible to produce different nanofibers with different compositions such as, *Phellinus igniarius* (Jiang et al., 2022), and multiple applications such as Piezoelectric Properties (Bai et al., 2022). On the other hand, it can mix a series of functional ingredients on the host polymers to form a functional composite or hybrid (Amini et al., 2022), which include little molecules (Kang et al., 2020), cells and bacterials (Pant, Tiwari), organic/inorganic nanoparticles (Zhao et al., 2021b) and MOFs (Zhu and Kim, 2022). Another capability of nanofibers is the synthesis of tri-layer nanodepots with various applications, including sustained release of acyclovir (Wang et al., 2020), fast helicide delivery (Liu et al., 2022). There have been reports on the use of nanofibers in the treatment of oral ulcers (Zhou et al., 2022) and other various applications in the fields of medicine, engineering, and environment (Sapountzi et al., 2020). The nature of nanofibers, which is a polymeric-shaped material, consists of various compounds with different configurations in controllable conditions. One of the most famous nanofibers is polysulfone (Ps) which has high thermal stability and mechanical strength, which can be used as insulation and reliable coatings (Choi et al., 2018; Alawady et al., 2020).

Metal-organic frameworks (MOF) are a novel class of nanomaterials that have many capabilities in different fields of engineering due to their significant porosity. These compounds, which are also compatible and biodegradable, can be used as novel adsorbent depending on the related conditions (Ren et al., 2015; Ding et al., 2019; Nimbalkar and Bhat, 2021).

MOFs can be combined with other compounds in a variety of procedures under different conditions. This feature facilized the performance of the final products in a potential area. One of the important properties expected to increase MOFs integration with other substrates, including SiO_2 nanoparticles, is the specific surface area. When MOFs combined with fibrous network immobilized by SiO_2 substrate, the porous nanostructures can expand in three-dimensional network with significant surface area (Zhan et al., 2012; Liu et al., 2019).

In order to integrate MOF with nanofibers and create a fibrous network, an electrospinning procedure was used (Gu et al., 2019; Liu et al., 2019). This method, which is fast, efficient, and cost-effective, not only produces uniform fibers but also affects the different properties of the product (Sarkar et al., 2010).

For systematic control of nanofibrous material, different procedure studies have been used. Compared to the classical methods, The application of novel organized routes can be affected the experimental parameters of the product and create stable compounds (Sargazi, Afzali, Mostafavi, Kazemian).

In the present study, for the first time, Ni-MOF/Ps nanofibrous networks were immobilized by SiO_2 substrate under optimal conditions of microwave assisted electrospinning method. The final products were characterized by transition electron microscopy (TEM), Fourier-transform infrared spectroscopy (FTIR), CHNSO elemental analysis, thermal stability analysis (TGA), and N_2 adsorption/desorption techniques. The compounds were used as novel material for CH_4 gas adsorption in optimal conditions.

2 Experimental

2.1 Reagents and instrumentation

Reagent-grade chemicals of nickel (iii) nitrate hexahydrate (Mw: 358.21 g/mol, 99.80%), and 2, 6- pyridine dicarboxylic acid (Mw: 167.12 g/mol, 99.85%) are purchased from Sigma. Ps and SiO_2 nanoparticles are purchased from Sigma Aldrich company. All products were commercially available and used without any further purification. The morphology and size distribution of Ni-MOF/Ps nanofibrous substrate was performed by TEM (Philips XL 30). FT-IR spectra were performed in transmission mode on a Nicolet AVATAR 360 FT-IR spectrophotometer using KBr powder as the sample matrix with a resolution of 4 cm^{-1}. TG behaviors were performed on a Mettler-Toledo TGA/SDTA851e. Adsorption isotherms were measured with an Autosorb 1-MP from Quantachrome Instruments.

2.2 Synthesis of Ni-MOF samples

In a typical microwave synthesis route, 0.063 g of $Ni(NO3)_3.5H_2O$ and 0.028 g of 2,6 pyridine-dicarboxylic acid were added in 50 ml distilled water. The solution was stirred for 50 min at 75°C. Then, the mixture was transfer into the microwave bath duration of 30 min at environment temperature.

2.3 Synthesis of Ni-MOF/Ps nanofibrous supported on SiO_2 substrate

For preparing the Ni-MOF/Ps nanofibers using microwave-assisted electrospinning method, the solutions obtained in Section 2.2 by microwave route were added into 0.5 g Ps with concentration (Ni-MOF) of 10 wt%. The solution was entered

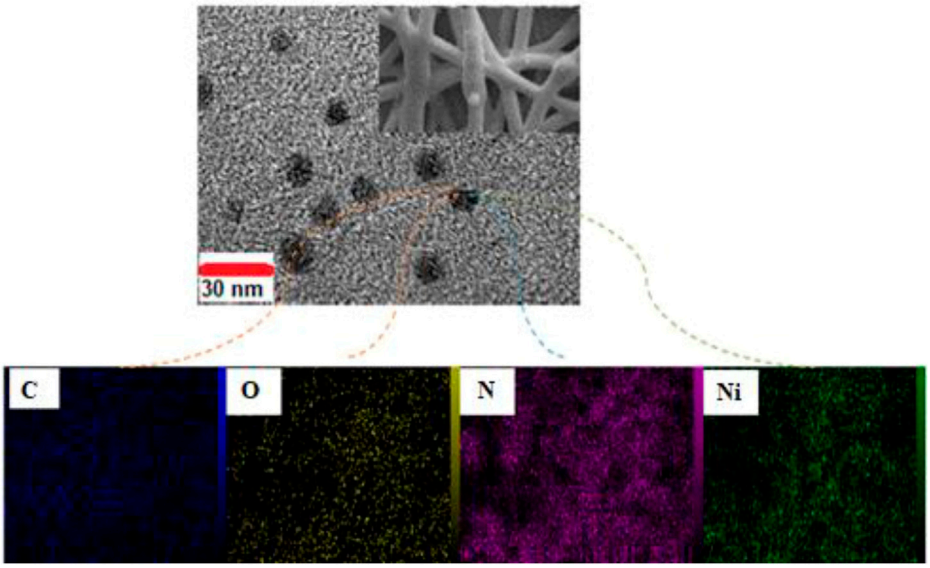

FIGURE 1
TEM image of Ni-MOF/Ps nanostructures supported on SiO_2 substrate with elemental mapping.

into the optimal electrospinning conditions, including applied voltages of 18 kV and the electrospinning distances of 12 cm. Also, the mixtures were injected from the syringe pump with flow rates of 0.15. After 2 h, the Ni-MOF/Ps nanofibrous polymer was isolated by calcination at 170°C. The 0.05 g of final products of Ni-MOF/Ps nanofibrous were added in 0.03 g of SiO_2 to obtain stable compounds of Ni-MOF/Ps nanofibrous.

3 Results and discussion

3.1 TEM with mapping analysis

Figure 1 shows TEM image of Ni-MOF/Ps fibrous nanostructures immobilized on SiO_2 nanoparticle which synthesized by microwave-assisted electrospinning method. Based on the results, this sample has a uniform morphology with a narrow fibrous size distribution about 25 nm (nanofibers have a dimension outside the nano range) (Zhang et al., 2021). The small size of nanofibers provides efficient conditions for their use in gas adsorption (Veerasimman et al., 2021). Also, based on this image, the Ni-MOF nanostructure was distributed in the nanofibrous network without any agglomeration in morphology. As a significant result, fibrous networks with Ni-MOF integration are well dispersed throughout the network. Also, the mapping analysis of Ni-MOF/Ps samples is shown in Figure 1. According to this Fig, Ni-MOF network was distributed on SiO_2 substrate which confirmed the successful synthesis of Ni-MOF/Ps fibrous nanostructures.

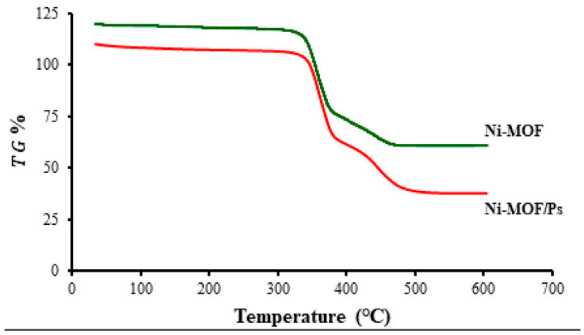

FIGURE 2
Thermal stability of Ni-MOF and Ni-MOF/Ps fibrous structures supported on SiO_2 substratev.

3.2 Thermal stability

TG analysis was used to evaluate the thermal stability performance of the Ni-MOF and Ni-MOF/Ps fibrous nanostructures supported on SiO_2 nanoparticles. Based on the results obtained from Figure 2, the Ni-MOF/Ps sample has good thermal stability than Ni-MOF (284°C compared to 261°C). The thermal stability of the nanostructures synthesized in this study has high thermal stability than previous compound due to physicho-chemical nature of this polymeric compound (Yang et al., 2019; Wu et al., 2022). This capability enables the efficiency of these nanostructures as efficient materials in the field of gas adsorption. One of the influential factors on thermal stability of

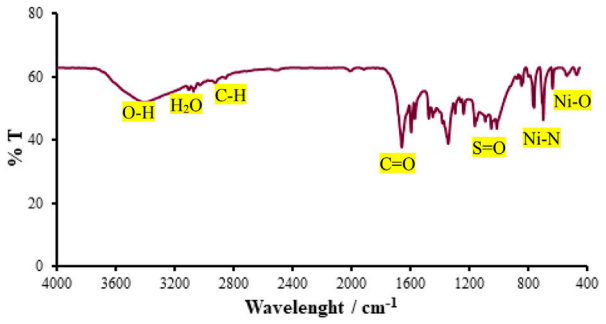

FIGURE 3
FTIR spectrum of Ni-MOF/Ps fibrous synthesized by microwave-assisted electrospinning procedure.

compounds is the application of electrospinning procedure as well as immobilization of Ni-MOF/Ps nanofibrous network by SiO_2 substrate (Irvin et al., 2019).

3.3 Suggested structures with elemental analysis

Figure 3 displays the FTIR spectrum of the Ni-MOF/Ps nanostructures synthesized by the microwave-assisted electrospinning method. The peak near 3390 cm^{-1} is assigned to the vibration of the carboxylic acid group (Nimbalkar and Bhat, 2021). The one about 3100 cm^{-1} showed the presence of coordinated water in the Ni-MOF/Ps sample, and the stretching vibration of aromatic C-H was observed around 2800 cm^{-1}. The peaks near 1600 cm^{-1} can be related to the stretching vibration of the -COO- groups in 2,6 pyridine dicarboxylic acid (ionized linker) (Ren et al., 2015; Hashemi et al., 2019). The peaks near 1100 cm^{-1} can be related to the stretching vibration of the–S=O- groups due to polysulfone. The peaks about 700 to 650 cm^{-1} and 540 cm^{-1} are related to the Ni-N and Ni-O bonds, respectively (Pietrzyk et al., 2021). According to FTIR spectra results and different configurations of the Ni-MOF with Ps, the final

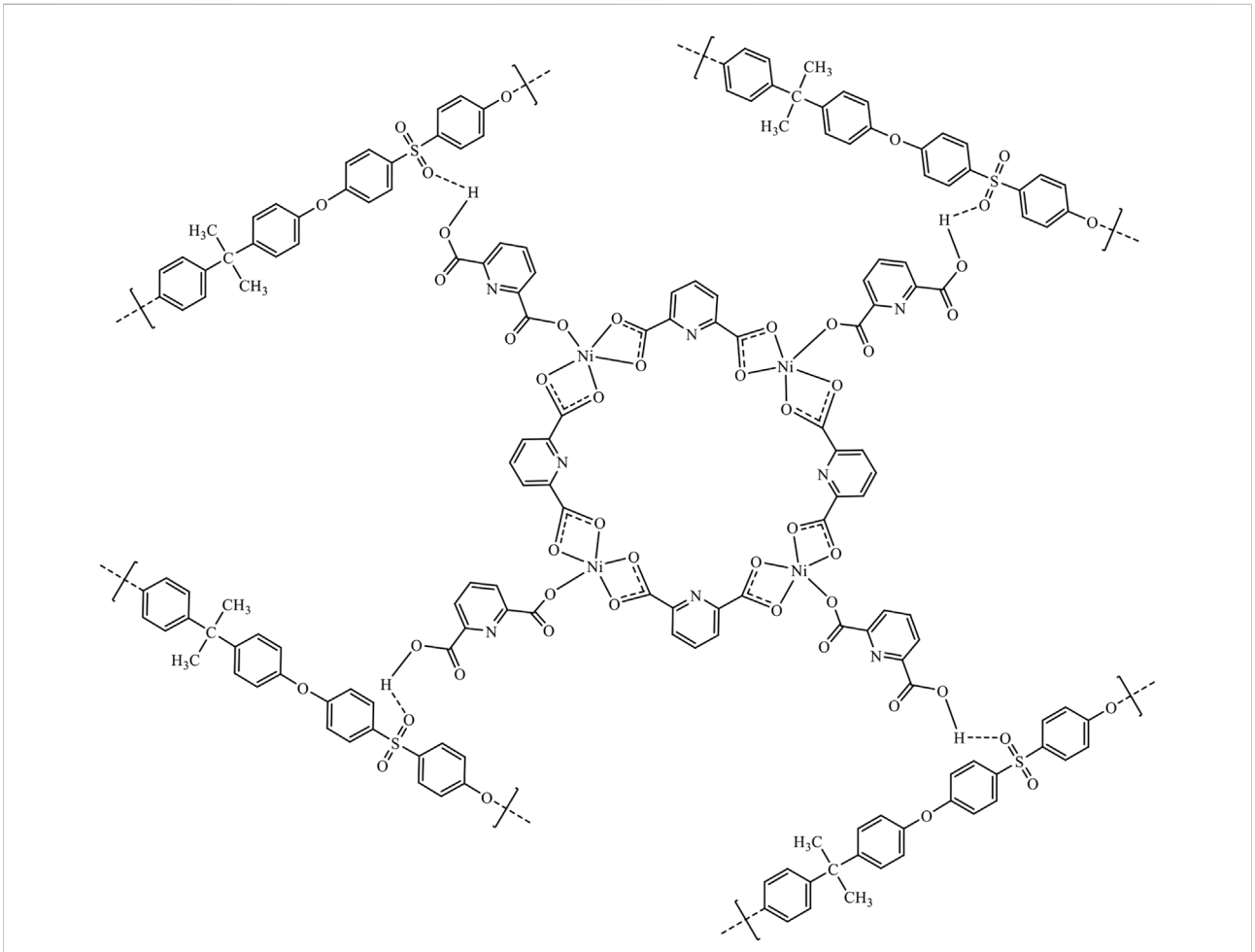

FIGURE 4
Proposed structures for Ni-MOF/Ps nafibrous polymers supported on SiO_2 substrate.

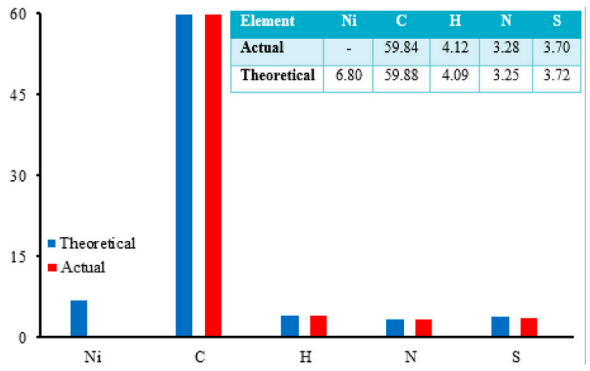

Element	Ni	C	H	N	S
Actual	-	59.84	4.12	3.28	3.70
Theoretical	6.80	59.88	4.09	3.25	3.72

FIGURE 5
CHNSO elemental analysis for Ni-MOF/Ps nanofibrous polymers.

structures of Ni-MOF/Ps fibrous samples were proposed in Figure 4. Also, CHNSO elemental analysis was used to determine the Ni-MOF/Ps fibrous nanostructures. Based on results obtained from Figure 5, the amount of Ni, O, C, N in the final structure not only presents the successful synthesis of Ni-MOF/Ps but also confirms the proposed structures of Figure 4.

3.4 Design of experiments

Since the specific surface area is an effective parameter for the interaction of nanofibers with the practical surface, the experimental design has been used to achieve the desired specific surface area. One of the influential factors proposed in previous studies is designing the electrospinning parameters. For this purpose, the voltage (a), concentration (b), and spinning distance (c) were selected. The fractional factorial method was used to design the experiment under different conditions. Table 1 shows the range of parameters as codded distribution. Table 2 also shows the fractional factorial design for the 10 experiments.

3.5 Systematic study

Figure 6 shows the residual plot for the specific surface area of Ni-MOF/Ps fibrous nanostructure supported on SiO_2 substrate. Based on the results, the distribution of the experiments is uniform, and there is no evidence of unscientific experiments. The effect of experimental parameters on the surface area is shown in Table 3. As it is known, all three parameters of voltage, concentration, and spinning distance affect the specific surface area (all parameters have a P_{value} close to 0.000) (Lakatta et al., 2010; Xiao et al., 2020; Lu et al., 2022).

TABLE 1 Coded levels and a range of experimental parameters for 2^{k-1} factorial design.

Level	Coded level		Uncoded level		
			Voltage (kV)	Concentration of PS (Wt)	Spinning distance (cm)
Low	−1	5	8	0.1	7
Center	0		16	0.2	12
High	+1	10	24	0.3	17

TABLE 2 Randomized complete fractional factorial design for surface area results.

Sample No.	Runs number	Std Order	a: Voltage (kV)	b: Concentration (Wt)	c: spinning distance (cm)	REP	Surface area (m^2/g)
I	1	5	−1	−1	−1	1	714
						2	712
II	2	3	0	0	0	1	1449
						2	1448
III	3	1	−1	0	−1	1	1320
						2	1320
IV	4	2	1	0	0	1	1690
						2	1692
V	4	4	1	−1	−1	1	985
						2	984

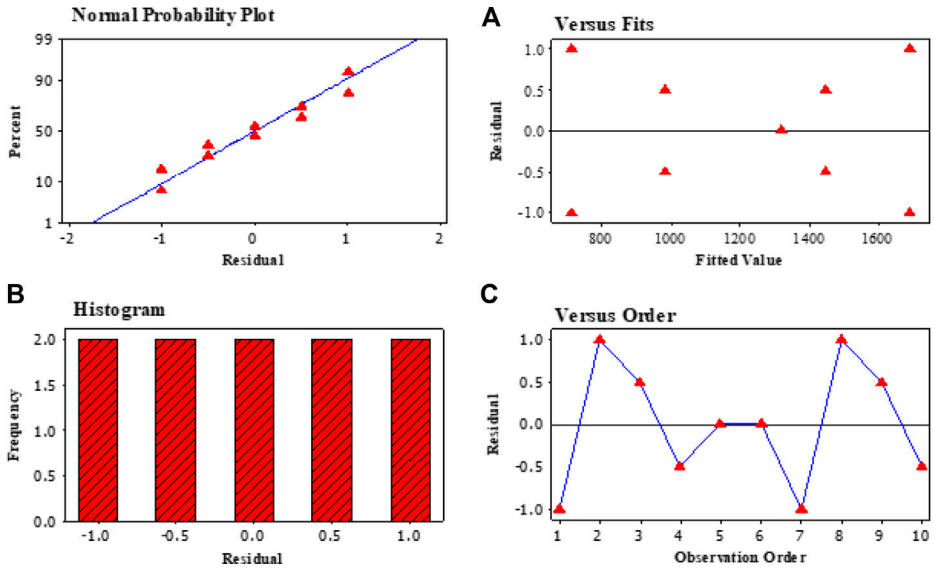

FIGURE 6
Residual plot for experimental parameters of voltage **(A)**, concentration **(B)** and spinning distance **(C)** on surface area.

TABLE 3 Analysis of variance in order to investigate the experimental parameters on surface area.

Source	DF	Seq SS	Adj SS	Adj MS	F	P_{value}
Main Effects	3	1182709	1118113	372704	372704.38	0.000
a	1	206403	58806	58806	3300.42	0.000
b	1	976140	291108	291108	1983.75	0.000
c	1	166	4332	4332	453.75	0.000
2-Way Interactions	1	9116	9116	9116	9116.45	0.000
Residual Error	5	5	5	1		

Previous studies have also confirmed the effect of voltage on the surface area of products. In fact, with increasing voltage, many electrical charges enter the sample, which results in increased efficiency of the electrospinning process.

Concentration also affects the specific surface area of the product by increasing the electric field. The distance between source and the collector is also a critical parameter affecting the final products' surface area. The distance between the source and the collector should be normal. In other words, increasing the spinning distance can make the fiber formation process more difficult. Also, by decreasing the distance between source and collector, the fibers are stretched less, and therefore their size distributions increases. As a significant result, the distance between the source and the collector should be standard rate. Also, as seen in Figure 7, the Pareto chart confirmed the considerable effects of experimental parameter (Voltage, Concentration, and Spinning distance) on surface area.

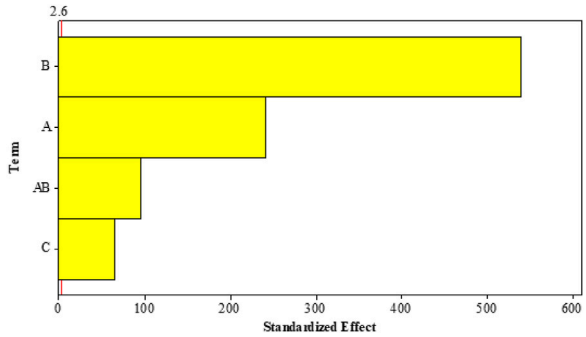

FIGURE 7
Pareto chart for investigate the effects of experimental parameters on surface area.

The adsorption/desorption isotherms of Ni-MOF/Ps fibrous polymer are shown in Figure 8. Based on the results obtained from this isotherm, sample IV has a similar adsorption/desorption behavior to the second classical isotherms, which indicates the structure of the microspores in this sample (Liu

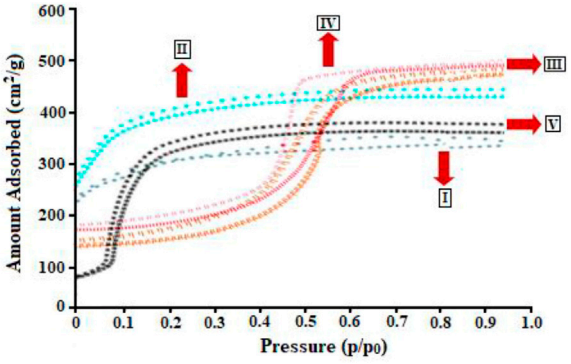

FIGURE 8
N_2 adsorption/desorption isotherm of Ni-MOF/Ps fibrous network synthesized under different conditions.

et al., 2017). Based on N_2 adsorption and desorption isotherm results, the sample IV has a larger surface area than other samples (1690 m^2/g). This unique surface not only distinguishes the nanostructure from the previous samples but also provides the necessary consistency for the application of final Ni-MOF/Ps fibrous polymeric productions in gas adsorption (Xue et al., 2020). Other samples' adsorption and desorption behavior also varies depending on the experimental conditions (see Table 2).

3.6 Optimization procedure

To systematic relationships between each of the experimental parameters on the surface area of Ni-MOF/Ps supported on SiO_2 substrate, three-dimensional plots have been used. As shown in Figure 9, by selecting each of the values of voltage (a), concentration (b), and spinning distance (c), different responses can be determined for the specific surface. This amount of equation is predicted based on the regression model (Dang et al., 2022; Zhao et al., 2022). The counter images also show the relationship between the experimental parameters to achieve optimal values (Figure 10). This particular level significantly affects Ni-MOF/Ps fibrous network applications.

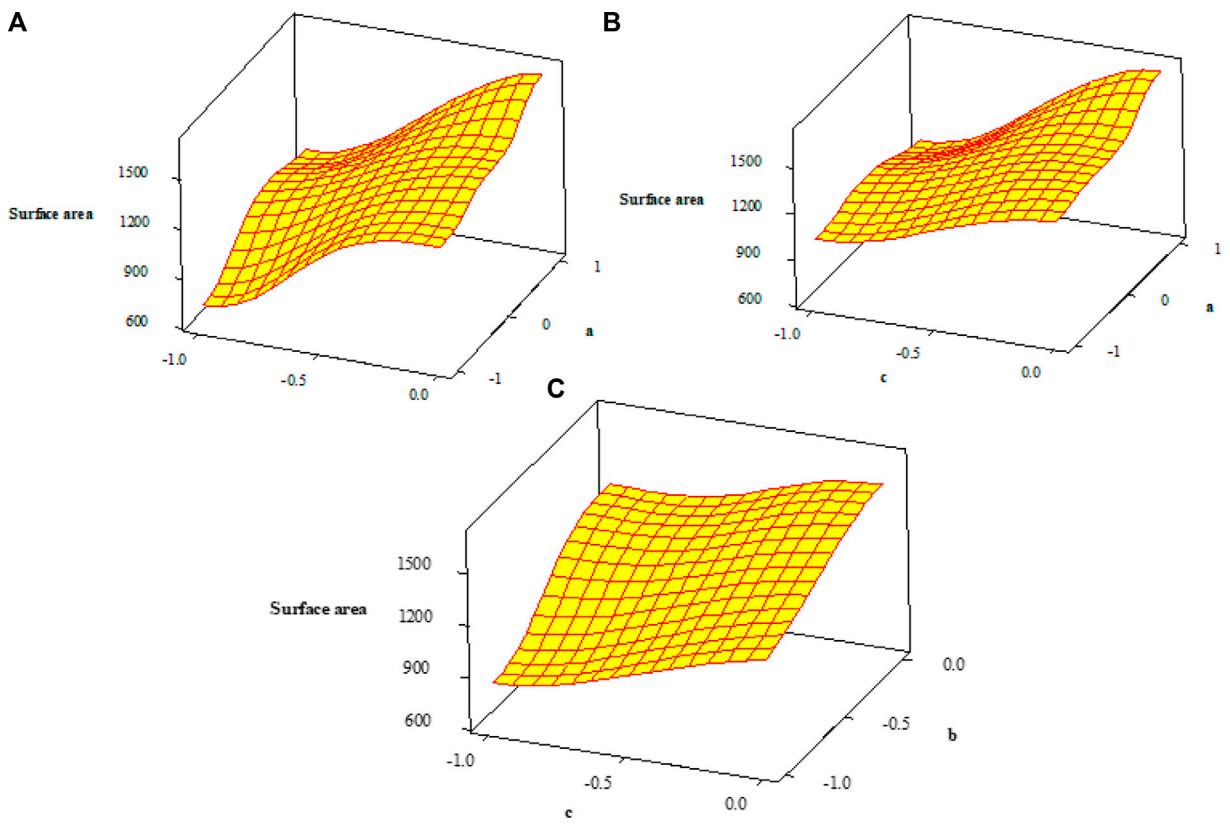

FIGURE 9
Surface plots for different experimental parameters [voltage **(A)**, concentration **(B)** and spinning distance **(C)**].

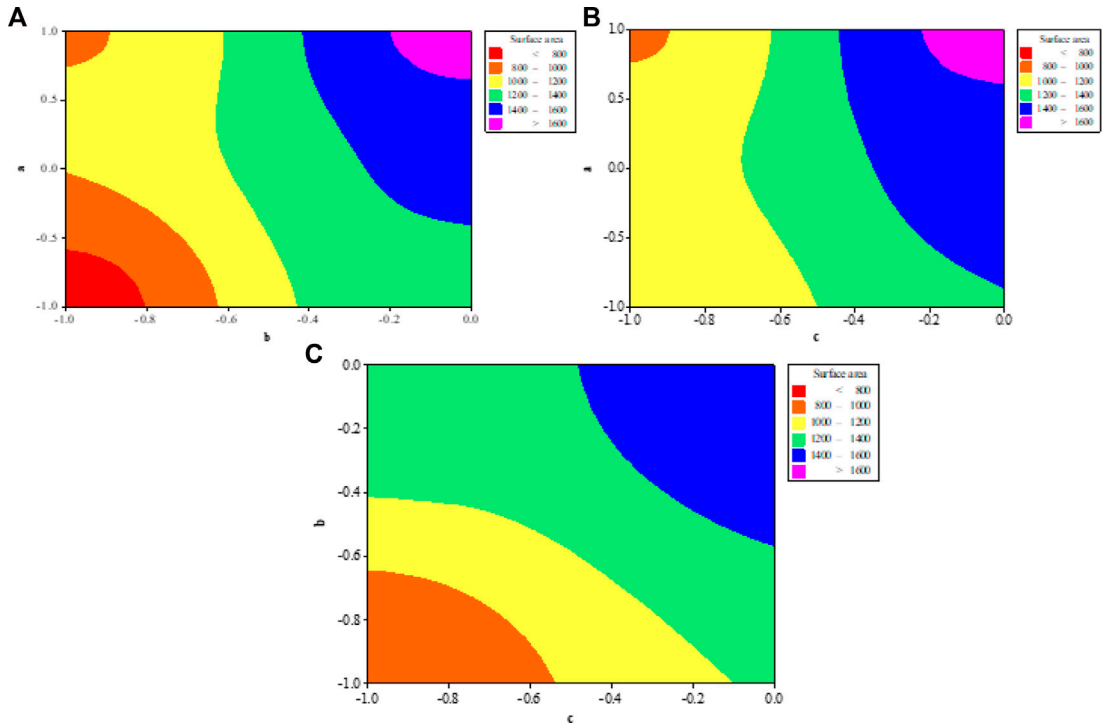

FIGURE 10
Contour plot of surface area *via* voltage **(A)**, concentration **(B)** and spinning distance **(C)**.

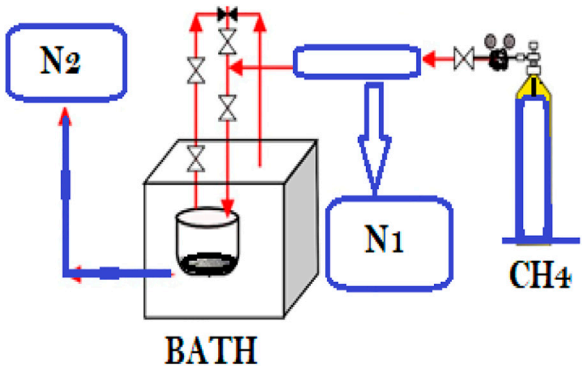

FIGURE 11
Schematic diagram of the experimental setup for measuring CH_4 adsorption.

3.7 CH_4 gas adsorption

According to the characterization results, Ni-MOF/Ps supported on SiO_2 substrate has been selected as the desirable sample with favorable physicochemical properties, therefore it has been used as a novel candidate for adsorption applications. In order to investigate adsorption properties, a volumetric reactor has been used. The purity of CH_4 gas adsorption was 99.99%.

To evaluate the CH_4 gas adsorption by Ni-MOF/Ps supported on SiO_2 substrate, a reactor setup composed of related parts is applies in Figure 11. First, a valve was installed between dozer (N1) and Tank (N2). Consequently, the number of CH_4 moles in the dozer was calculated using Eq. 1:

$$P_1V_1 = Z_1N_1RT \Rightarrow N1 = \frac{P1V1}{Z1RT} \quad (1)$$

Where P_1, N_1, R, T, and Z_1 show gas pressure, number of CH_4 gas moles, general constant of gases, equilibrium temperature, and compressibility coefficient, respectively. At the second step, the number of the gas moles in tank could be calculated by Eq. 2:

$$P_2V_2 = Z_2N_2RT \Rightarrow N2 = \frac{P2V2}{Z2RT} \quad (2)$$

Where P_2, Z_2, and V_2 indicate gas pressure, compressibility coefficient factor in the adsorption reservoir, and total volume of the gas adsorption. Finally, the gas moles adsorbed by Ni-MOF/Ps supported on SiO_2 substrate could be calculated by $n_{ADS} = n_1\text{-}n_2$. The compressibility factor (Z_1, Z_2) was calculated based on methodology of literature (Sargazi et al., 2019).

The results show that the sample has an adsorption rate of about 5.14 mmoL/g. This amount of adsorption has increased significantly compared to other adsorbents.

The high activity of Ni-MOF/polysulfide fibrous nanostructure, as compared to activated carbon and Zeolite, may be ascribed to the greater surface area, the type of substrate and the microwave synthesis method, which may ensure the high dispersion of palladium active sites and facilitate the diffusion of reactants and large product molecules in the pore. It seems that the type of substrate used, the type of composite adsorbents and the microwave synthesis method have a great impact on the properties of these samples.

4 Conclusion

In this study, for the first time, Ni-MOF/Ps nanofibers have been supported on SiO_2 substrate using an efficient and fast microwave-assisted electrospinning procedure under optimal conditions. Various techniques have been used to characterize the resulting samples. TEM image showed that the samples have an average diameter about 25 nm. TGA analysis and BET techniques showed that the Ni-MOF/Ps nanofibrous polymer immobilized on SiO_2 substrate had thermal stability of 284°C and a specific surface area of 1690 m^2/g, respectively. A fractional factorial design technique has been used to obtain the desired properties. This systematically showed that the experimental parameters of voltage, concentration, and spinning distance greatly affect the surface of the sample. The synthesis of fibrous samples with biocompatible and biodegradable properties and excellent particular surface area makes their use as a new option for CH_4 gas adsorption. The developed method developed in this study can be extended for producing efficient adsorbent materials with a high reversible capacities and performance capabilities for diverse application.

Data availability statement

The raw data supporting the conclusions of this article will be made available by the authors, without undue reservation.

Author contributions

All authors listed have made a substantial, direct, and intellectual contribution to the work and approved it for publication.

Acknowledgments

The authors extend their appreciation to the Deputyship for Research & Innovation, Ministry of Education in Saudi Arabia for funding this research work through the project number (IF2/PSAU/2022/01/22681).

Conflict of interest

The authors declare that the research was conducted in the absence of any commercial or financial relationships that could be construed as a potential conflict of interest.

Publisher's note

All claims expressed in this article are solely those of the authors and do not necessarily represent those of their affiliated organizations, or those of the publisher, the editors and the reviewers. Any product that may be evaluated in this article, or claim that may be made by its manufacturer, is not guaranteed or endorsed by the publisher.

References

Alawady, A. R., Alshahrani, A. A., Aouak, T. A., and Alandis, N. M. (2020). Polysulfone membranes with CNTs/Chitosan biopolymer nanocomposite as selective layer for remarkable heavy metal ions rejection capacity. *Chem. Eng. J.* 388, 124267. doi:10.1016/j.cej.2020.124267

Amini, A., Kazemzadeh, P., Jafari, M., Moghaddam-Manesh, M., Pal Singh Chauhan, N., Fazelian, N., et al. (2022). Fabrication of fibrous materials based on cyclodextrin and egg shell waste as an affordable composite for dental applications *Front. Med.* doi:10.3389/fmats.2022.919935

Bai, Y., Liu, Y., Lv, H., Shi, H., Zhou, W., Liu, Y., et al. (2022). Processes of electrospun polyvinylidene fluoride-based nanofibers, their piezoelectric properties, and several fantastic applications. *Polymers* 14, 4311. doi:10.3390/polym14204311

Choi, S.-W., Kim, T.-H., Jo, S.-W., Lee, J. Y., Cha, S.-H., and Hong, Y. T. (2018). Hydrocarbon membranes with high selectivity and enhanced stability for vanadium redox flow battery applications: Comparative study with sulfonated poly (ether sulfone) s and sulfonated poly (thioether ether sulfone) s. *Electrochimica Acta* 259, 427–439. doi:10.1016/j.electacta.2017.10.121

Conte, G., Stelitano, S., Policicchio, A., Minuto, F. D., Lazzaroli, V., Galiano, F., et al. (2020). Assessment of activated carbon fibers from commercial Kevlar® as nanostructured material for gas storage: Effect of activation procedure and adsorption of CO2 and CH4. *J. Anal. Appl. Pyrolysis* 152, 104974. doi:10.1016/j.jaap.2020.104974

Dang, W., Guo, J., Liu, M., Liu, S., Yang, B., Yin, L., et al. (2022). A semi-supervised extreme learning machine algorithm based on the new weighted kernel for machine smell. *Appl. Sci.* 12, 9213. doi:10.3390/app12189213

Ding, M., Cai, X., and Jiang, H.-L. (2019). Improving MOF stability: Approaches and applications. *Chem. Sci.* 10, 10209–10230. doi:10.1039/c9sc03916c

Fischer, M. (2018). *Präklinische Untersuchungen zum Einfluss von Wundauflagen aus bakteriellem Alginat auf Entzündungsmediatoren und Keiminaktivierung.* Universität Ulm.Washington, D.C, USA

Glencross, D. A., Ho, T.-R., Camina, N., Hawrylowicz, C. M., and Pfeffer, P. E. (2020). Air pollution and its effects on the immune system. *Free Radic. Biol. Med.* 151, 56–68. doi:10.1016/j.freeradbiomed.2020.01.179

Gu, W., Lv, J., Quan, B., Liang, X., Zhang, B., and Ji, G. (2019). Achieving MOF-derived one-dimensional porous ZnO/C nanofiber with lightweight and enhanced microwave response by an electrospinning method. *J. Alloys Compd.* 806, 983–991. doi:10.1016/j.jallcom.2019.07.334

Han, M.-C., Cai, S.-Z., Wang, J., and He, H.-W. (2022). Single-side superhydrophobicity in Si3N4-doped and SiO2-treated polypropylene nonwoven webs with antibacterial activity. *Polymers* 14, 2952. doi:10.3390/polym14142952

Hashemi, S. H., Kaykhaii, M., Keikha, A. J., Mirmoradzehi, E., and Sargazi, G. (2019). Application of response surface methodology for optimization of metal–organic framework based pipette-tip solid phase extraction of organic dyes from seawater and their determination with HPLC. *BMC Chem.* 13, 59–10. doi:10.1186/s13065-019-0572-0

Irvin, C. W., Satam, C. C., Meredith, J. C., and Shofner, M. L. (2019). Mechanical reinforcement and thermal properties of PVA tricomponent nanocomposites with chitin nanofibers and cellulose nanocrystals. *Compos. Part A Appl. Sci. Manuf.* 116, 147–157. doi:10.1016/j.compositesa.2018.10.028

Jerrett, M., Arain, A., Kanaroglou, P., Beckerman, B., Potoglou, D., Sahsuvaroglu, T., et al. (2005). A review and evaluation of intraurban air pollution exposure models. *J. Expo. Sci. Environ. Epidemiol.* 15, 185–204. doi:10.1038/sj.jea.7500388

Jiang, W., Zhang, X., Liu, P., Zhang, Y., Song, W., Yu, D.-G., et al. (2022). Electrospun healthcare nanofibers from medicinal liquor of Phellinus igniarius. *Adv. Compos. Hybrid Mater.* 5, 3045–3056. doi:10.1007/s42114-022-00551-x

Kang, S., Hou, S., Chen, X., Yu, D., Wang, L., Li, X., et al. (2020). Energy-saving electrospinning with a concentric teflon-core rod spinneret to create medicated nanofibers. *Polymers* 12, 2421. doi:10.3390/polym12102421

Karimi, M., Rodrigues, A. E., and Silva, J. A. (2021). Designing a simple volumetric apparatus for measuring gas adsorption equilibria and kinetics of sorption. Application and validation for CO2, CH4 and N2 adsorption in binder-free beads of 4A zeolite. *Chem. Eng. J.* 425, 130538. doi:10.1016/j.cej.2021.130538

Klewiah, I., Berawala, D. S., Walker, H. C. A., Andersen, P. Ø., and Nadeau, P. H. (2020). Review of experimental sorption studies of CO2 and CH4 in shales. *J. Nat. Gas Sci. Eng.* 73, 103045. doi:10.1016/j.jngse.2019.103045

Lakatta, E. G., Maltsev, V. A., and Vinogradova, T. M. (2010). A coupled SYSTEM of intracellular Ca2+ clocks and surface membrane voltage clocks controls the timekeeping mechanism of the heart's pacemaker. *Circulation Res.* 106, 659–673. doi:10.1161/circresaha.109.206078

Liu, G., Li, L., Xu, D., Huang, X., Xu, X., Zheng, S., et al. (2017). Metal–organic framework preparation using magnetic graphene oxide–β-cyclodextrin for neonicotinoid pesticide adsorption and removal. *Carbohydr. Polym.* 175, 584–591. doi:10.1016/j.carbpol.2017.06.074

Liu, H., Wang, H., Lu, X., Murugadoss, V., Huang, M., Yang, H., et al. (2022). Electrospun structural nanohybrids combining three composites for fast helicide delivery. *Adv. Compos. Hybrid Mater.* 5, 1017–1029. doi:10.1007/s42114-022-00478-3

Liu, M., Cai, N., Chan, V., and Yu, F. (2019). Development and applications of MOFs derivative one-dimensional nanofibers via electrospinning: A mini-review. *Nanomaterials* 9, 1306. doi:10.3390/nano9091306

Lu, S., Guo, J., Liu, S., Yang, B., Liu, M., Yin, L., et al. (2022). An improved algorithm of drift compensation for olfactory sensors. *Appl. Sci.* 12, 9529. doi:10.3390/app12199529

Nazar, W., and Niedoszytko, M. (2022). Air pollution in Poland: A 2022 narrative review with focus on respiratory diseases. *Int. J. Environ. Res. Public Health* 19, 895.

Nimbalkar, M. N., and Bhat, B. R. (2021). Simultaneous adsorption of methylene blue and heavy metals from water using Zr-MOF having free carboxylic group. *J. Environ. Chem. Eng.* 9, 106216. doi:10.1016/j.jece.2021.106216

Okolo, G. N., Everson, R. C., Neomagus, H. W., Roberts, M. J., and Sakurovs, R. (2015). Comparing the porosity and surface areas of coal as measured by gas adsorption, mercury intrusion and SAXS techniques. *Fuel* 141, 293–304. doi:10.1016/j.fuel.2014.10.046

Pant, H. R., and Tiwari, A. P. Electrospinning based functional scaffolds for biomedical applications. *Front. Mater.*, 406.

Pietrzyk, P., Góra-Marek, K., Mazur, T., Mozgawa, B., Radoń, M., Chiesa, M., et al. (2021). Structure and mechanistic relevance of Ni2+–NO adduct in model HC SCR reaction over NiZSM-5 catalyst–Insights from standard and correlation EPR and IR spectroscopic studies corroborated by molecular modeling. *J. Catal.* 394, 206–219. doi:10.1016/j.jcat.2020.07.018

Ren, J., Langmi, H. W., North, B. C., and Mathe, M. (2015). Review on processing of metal–organic framework (MOF) materials towards system integration for hydrogen storage. *Int. J. Energy Res.* 39, 607–620. doi:10.1002/er.3255

Sapountzi, E., Chateaux, J.-F., and Lagarde, F. (2020). Combining electrospinning and vapor-phase polymerization for the production of polyacrylonitrile/polypyrrole core-shell nanofibers and glucose biosensor application. *Front. Chem.* 8, 678. doi:10.3389/fchem.2020.00678

Sargazi, G., Afzali, D., Mostafavi, A., and Kazemian, H. (2020). A novel composite derived from a metal organic framework immobilized within electrospun nanofibrous polymers: An efficient methane adsorbent. *Appl. Organomet. Chem.* 34, e5448. doi:10.1002/aoc.5448

Sargazi, G., Afzali, D., Mostafavi, A., Shadman, A., Rezaee, B., Zarrintaj, P., et al. (2019). Chitosan/polyvinyl alcohol nanofibrous membranes: Towards green super-adsorbents for toxic gases. *Heliyon* 5, e01527. doi:10.1016/j.heliyon.2019.e01527

Sarkar, K., Gomez, C., Zambrano, S., Ramirez, M., de Hoyos, E., Vasquez, H., et al. (2010). Electrospinning to Forcespinning™. *Electrospinning forcespinning™, Mater. today* 13, 12–14. doi:10.1016/s1369-7021(10)70199-1

Veerasimman, A., Shanmugam, V., Rajendran, S., Johnson, D. J., Subbiah, A., Koilpichai, J., et al. (2021). Thermal properties of natural fiber sisal based hybrid composites–A brief review. *J. Nat. Fibers* 19, 4696–4706. doi:10.1080/15440478.2020.1870619

Wang, M., Hou, J., Yu, D.-G., Li, S., Zhu, J., and Chen, Z. (2020). Electrospun tri-layer nanodepots for sustained release of acyclovir. *J. Alloys Compd.* 846, 156471. doi:10.1016/j.jallcom.2020.156471

Wu, R., Tan, Y., Meng, F., Zhang, Y., and Huang, Y.-X. (2022). PVDF/MAF-4 composite membrane for high flux and scaling-resistant membrane distillation. *Desalination* 540, 116013. doi:10.1016/j.desal.2022.116013

Xiao, Y., Zuo, X., Huang, J., Konak, A., and Xu, Y. (2020). The continuous pollution routing problem. *Appl. Math. Comput.* 387, 125072. doi:10.1016/j.amc.2020.125072

Xue, X., Qiu, M., Li, Y., Zhang, Q., Li, S., Yang, Z., et al. (2020). Creating an eco-friendly building coating with smart subambient radiative cooling. *Adv. Mater.* 32, 1906751. doi:10.1002/adma.201906751

Yang, Y., Wang, S. Q., Wen, H., Ye, T., Chen, J., Li, C. P., et al. (2019). Nanoporous gold embedded ZIF composite for enhanced electrochemical nitrogen fixation. *Angew. Chem. Int. Ed.* 58, 15506–15510. doi:10.1002/ange.201909770

Zhan, Y., Liu, Z., Najmaei, S., Ajayan, P. M., and Lou, J. (2012). Large-area vapor-phase growth and characterization of MoS2 atomic layers on a SiO2 substrate. *Small* 8, 966–971. doi:10.1002/smll.201102654

Zhang, X., Shi, X., Gautrot, J. E., and Peijs, T. (2021). Nanoengineered electrospun fibers and their biomedical applications: A review. *Nanocomposites* 7, 1–34. doi:10.1080/20550324.2020.1857121

Zhao, C., Xi, M., Huo, J., and He, C. (2021). B-Doped 2D-InSe as a bifunctional catalyst for CO 2/CH 4 separation under the regulation of an external electric field. *Phys. Chem. Chem. Phys.* 23, 23219–23224.

Zhao, C., Xi, M., Huo, J., He, C., and Fu, L. (2023). Computational design of BC3N2 based single atom catalyst for dramatic activation of inert CO2 and CH4 gasses into CH3COOH with ultralow CH4 dissociation barrier. *Chin. Chem. Lett.* 34, 107213. doi:10.1016/j.cclet.2022.02.018

Zhao, K., Lu, Z.-H., Zhao, P., Kang, S.-X., Yang, Y.-Y., and Yu, D.-G. (2021). Modified tri–axial electrospun functional core–shell nanofibrous membranes for natural photodegradation of antibiotics. *Chem. Eng. J.* 425, 131455. doi:10.1016/j.cej.2021.131455

Zhao, S., Li, H., Wang, B., Yang, X., Peng, Y., Du, H., et al. (2022). Recent advances on syngas conversion targeting light olefins. *Fuel* 321, 124124. doi:10.1016/j.fuel.2022.124124

Zhou, Y., Wang, M., Yan, C., Liu, H., and Yu, D.-G. (2022). Advances in the application of electrospun drug-loaded nanofibers in the treatment of oral ulcers. *Biomolecules* 12, 1254. doi:10.3390/biom12091254

Zhu, X., and Kim, K. (2022). Electrospun polyacrylonitrile fibrous membrane for dust removal. *Front. Mater.* 9, 973660. doi:10.3389/fmats.2022.973660

Zuo, W., Zhang, W., Liu, Y., Han, H., Huang, C., Jiang, W., et al. (2022). *Pore structure characteristics and adsorption and desorption capacity of coal rock after exposure to clean fracturing fluid*. ACS Omega.Wurttemberg, Germany